Supplementary Information

An Electric Field–Based Approach for Quantifying Effective Volumes and Radii of Chemically Affected Space

Austin M. Mroz, Audrey M. Davenport, Jasper Sterling, Joshua Davis, Christopher H. Hendon*

Department of Chemistry and Biochemistry, University of Oregon, Eugene, OR, 97403

Email: chendon@uoregon.edu

STREUSEL release, v2022:

DOI: 10.5281/zenodo.6459535

Link to STREUSEL github code:

https://github.com/hmsoregon/STREUSEL

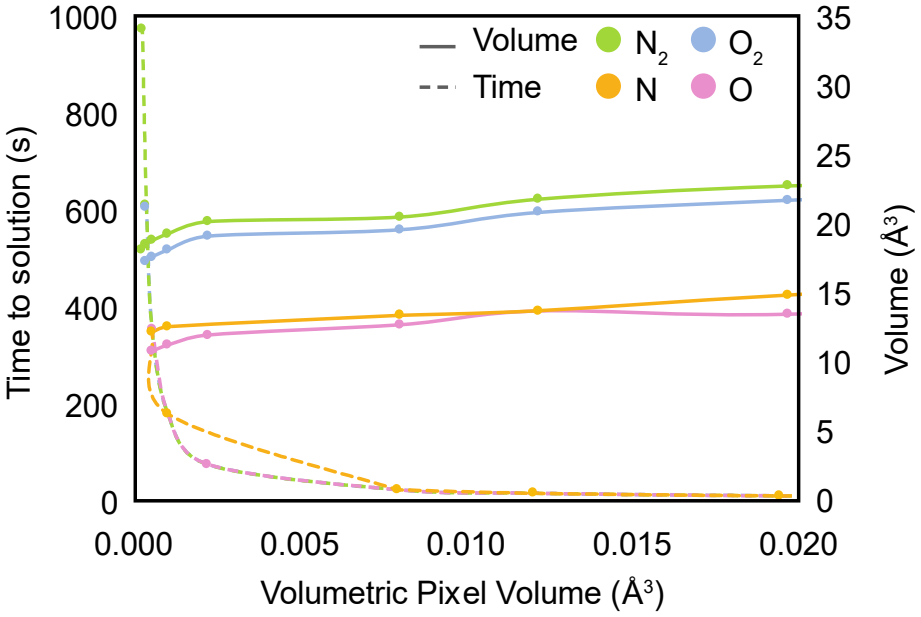

Figure S1. Decreasing the voxel increases the time to solution (dashed curves) exponentially yet maximizes the accuracy of the calculated volume (solid curves). CCSD-full/aug-cc-pvTZ.

Volumetric pixel (voxel) resolution

The electrostatic potential tensors are extracted from the Gaussian09 optimization calculations. The dimension of the tensor (number of elements per side) and the length (in Euclidian space) of each side is variable; the resolution is best represented as the real space volume that each element in the tensor represents (holding the total length of the computational box constant). At large voxel volume (> 0.02 A^3), the volume approaches notable fractions of bond lengths (i.e. too low resolution), resulting in artificially large calculated volumes.

To identify the optimal resolution (maximizing the voxel volume, while minimizing the time to solution) the time to solution and calculated volumes were calculated for four representative models (N_2, O_2, N, and O), Figure S2.

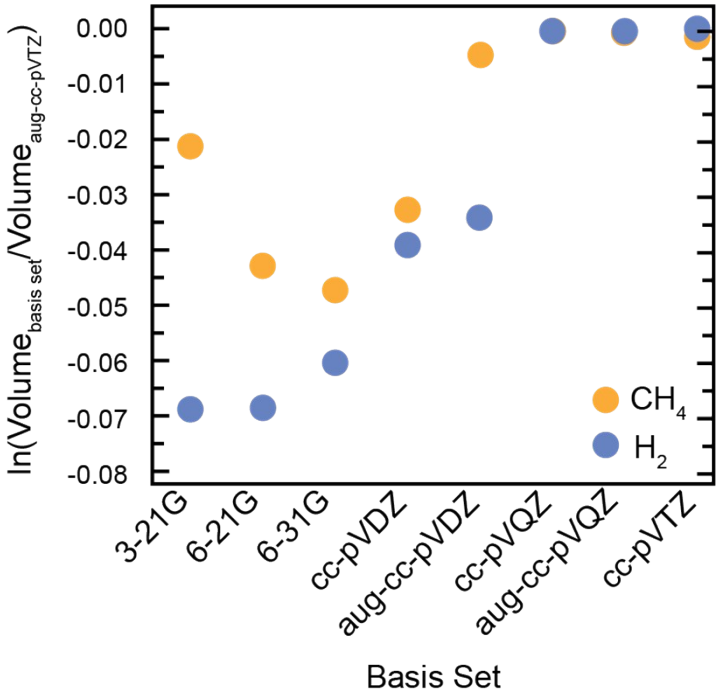

Figure S2. Calculated STREUSEL volumes of H_2 and CH_4 optimized with each basis set (x-axis), normalized to the volume obtained from the aug-cc-pVTZ (y-axis). The normalized volumes represent the precision of each basis set, a metric of how close the returned electronic structure is to that obtained using aug-cc-pVTZ. aug-cc-pVTZ is considered sufficiently large – as demonstrated by the convergence of normalized volumes with larger basis sets (*i.e.* cc-pVQZ and aug-cc-pVQZ).

Mg Atomic and Ionic Radii Comparisons

Table S1. Comparison of radii (Å) for Mg in three oxidation states (Mg, Mg^{+}, and Mg^{2+}). STREUSEL data obtained using CCSD-full/aug-cc-pVTZ.

	Radii Type/Method	Coordination Number	Radii (Å) Mg	Mg^{+}	Mg^{2+}
Pyykkö[1,2]	Single Covalent		1.39		
	Double Covalent		1.32		
	Triple Covalent		1.27		
	Tetrahedral		1.41		
Alvarez[3,4]	Non-bonded		2.51		
	Covalent		1.41		
Bragg[5]			1.42		
Slater[6]			1.50		
Bondi[7,8]			1.73		
Rahm[9]	Electron Density	*I*[a]	2.40	2.01	
Batsanov[10]		8	2.20		0.89
		12	1.60		1.23
Shannon-Prewitt[11,12]	Effective ionic	6			0.72
	Crystal	6			0.86
Ouyang[13]		12			1.15
Agmon[14]					0.69
Pauling[15]					0.65
STREUSEL	Electric Field	*I*[a]	2.15	2.83	3.74

[a] Independent of coordination number

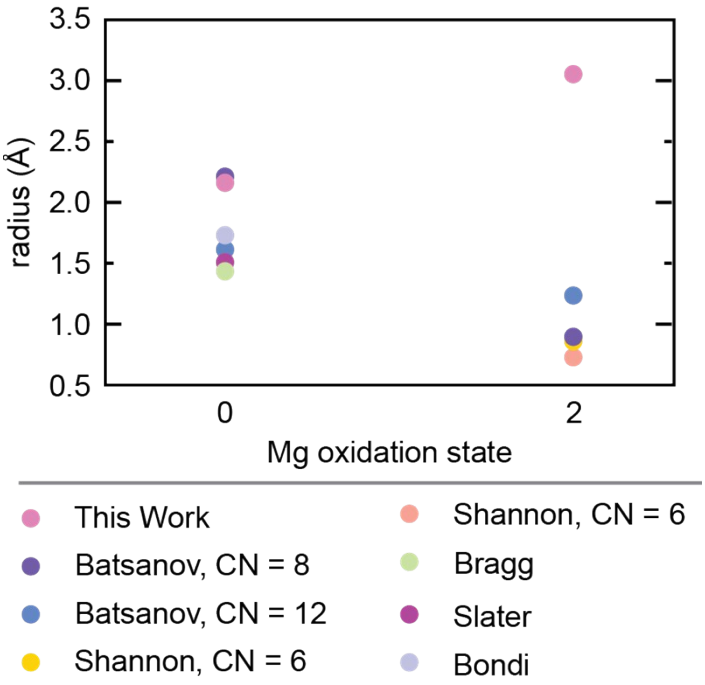

Figure S3. Radii (y-axis) of Mg in two oxidation states (x-axis) for a series of experimental size methods (CN = coordination number). All conventional volumetric approaches predict cations to be smaller than their neutral counterparts, because other approaches are based on electron density. STREUSEL data obtained using CCSD-full/aug-cc-pVTZ.

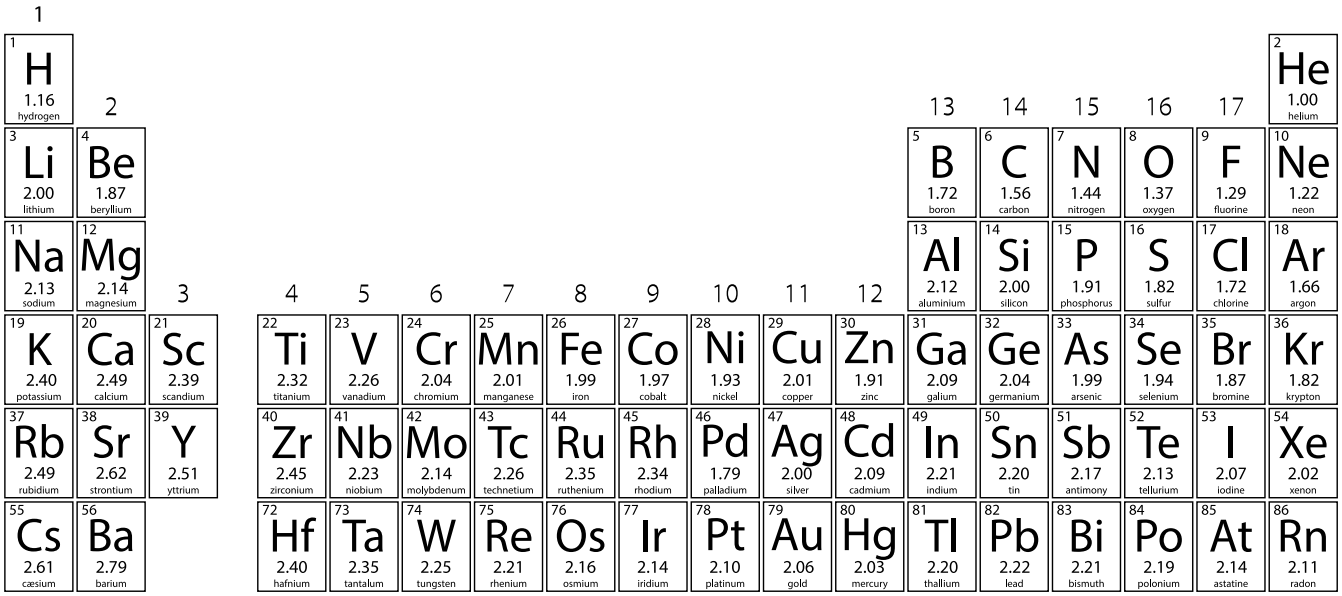

Figure S4 Atomic radii for elements 1-96 of the periodic table calculated using STREUSEL are presented. Neutral atoms were modeled using functional CCSD-full with the def2-TZVP basis set. The radii are calculated from the STREUSEL-obtained volumes under the spherical approximation.

Table S2. Atomic radius from STREUSEL as a function of basis set. CCSD-full was used in both cases. The radii vary by a maximum of 0.4%.

	def2-TZVP	aug-cc-pVTZ
Sc	**2.39**	**2.40**
Ti	**2.32**	**2.31**
V	**2.26**	**2.27**
Cr	**2.04**	**2.03**
Mn	**2.01**	**2.01**
Fe	**1.99**	**1.99**
Co	**1.97**	**1.97**
Ni	**1.93**	**1.93**
Cu	**2.01**	**2.01**
Zn	**1.98**	**1.99**

Overlapping sphere volume calculation (any radii may be used, assuming spheres do not change shape, just further penetrate into one another)

Chemical volumes using rigid spheres are a function of the volumes of each of the atoms ($v_x,\ x = a,b$), which are reliant on the selected method's reported radii ($r_x, x = a,b$)

$$v_x = \frac{4}{3}\pi r_x^3 \qquad (5)$$

and the overlap between the rigid spheres (o_d), which relies on the reported radii of each of the atoms (r_x, $x = a,b$) and the distance between them (d_{ab})

$$o_d = \frac{\pi(r_a + r_b - d_{ab})(d_{ab}^2 + 2d_{ab}r_a - 3r_a^2 + 2d_{ab}r_b + 6r_a r_b - 3r_b^2)}{12d_{ab}} \qquad (6)$$

Thus, the total volume can be written

$$v_{vdW} = \sum_{i=1}^{n}\frac{4}{3}\pi r_i^3 - \sum_{a=1}^{n}\sum_{b=1}^{n}\frac{\pi(r_a + r_b - d_{ab})(d_{ab}^2 + 2d_{ab}r_a - 3r_a^2 + 2d_{ab}r_b + 6r_a r_b - 3r_b^2)}{12d_{ab}} \qquad (7)$$

The relationship between, in this case, van der Waals volumes and changing bond lengths is readily examined using diatomic molecules. Both homonuclear and heteronuclear diatomic molecules exhibit the same trend in calculated van der Waals volume upon changing bond length. Intuitively, there is a direct relationship between bond length and volume derived using rigid spheres.

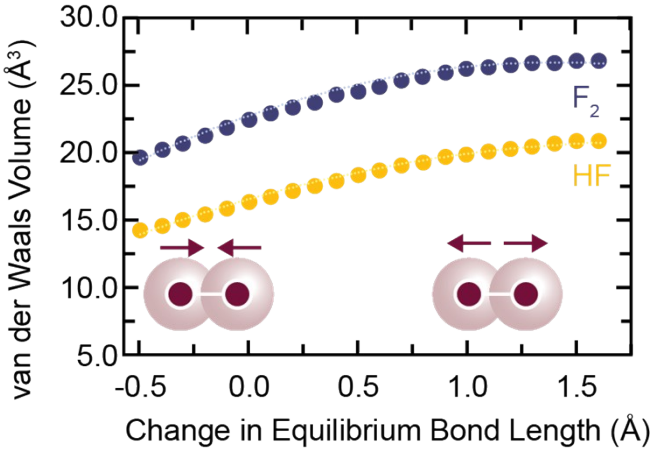

Figure S5. van der Waals volumes (y-axis) of F_2 and HF were calculated for the optimized structures, and a series of models with expanded and compressed bond lengths (x-axis).

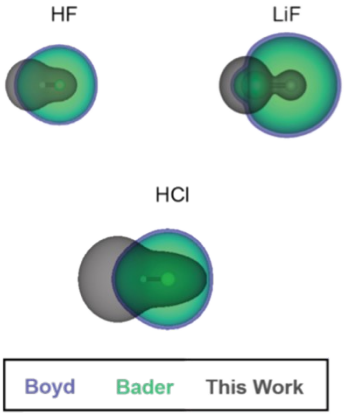

Figure S6. The Boyd (periwinkle), Bader (mint), and STREUSEL (charcoal) surfaces of a series of diatomic molecules. All surfaces are plotted using VESTA. The Boyd surface is depicted at an isosurface value of 0.00015 $e^{-}Å^{-3}$. The Bader surface is depicted at an isosurface value of 0.0003 $e^{-}Å^{-3}$. The STREUSEL surface is depicted at an isosurface value relative to the minimum value of the electric field surface mapped on the electrostatic potential map. STREUSEL volumes computed using CCSD-full/aug-cc-pVTZ.

Atom and small molecule calculations

Density functional theory (DFT) was used to perform geometry optimizations for the atoms and small molecules of interest, as implemented in Gaussian09.[17] Optimizations were performed using a RMS force convergence of 10^{-5} hartree. The electronic wavefunction was minimized using representative functionals from each level of theory, Table S2, with a triple zeta basis set, including polarization and diffuse functions on all atoms.[18] All calculations were performed using a triple zeta polarized basis. Aug-cc-pVTZ was used when possible (for elements up to Kr), otherwise def2-TZVP was employed. CCSD-full was used as our reference for the exact solution.

Table S3. Several representative functionals from each level of theory (*ab initio*, generalized gradient exchange (GGE), local-density approximation (LDA), range separated, generalized gradient approximation (GGA), hybrid-GGA (H-GGA), hybrid-meta-GGA (HM-GGA), and meta-GGA (M-GGA).

Ab initio	GGE	LDA	Range Separated
CCSD-full[19–22]	BVWN5[23,24]	Xalpha[25–27]	wB97XD[28]
MP3[29,30]	G96VWN5[24,31]	LSDA[24–27]	CAM-B3LYP[18]
MP4[32,33]	OVWN5[24,34,35]	SVWN5[24–27]	

GGA	H-GGA	HM-GGA	M-GGA
PBE[36,37]	APFD[38]	B1B95[23]	M06L[39]
B97d[40]	B1LYP[23,41,42]	BMK[43]	M11L[44]
BLYP[23,41,42]	B3LYP[23,41,42]	TPSSh[45–47]	TPSS[45]
BPBE[23,36,37]	B3P86[23]		VSXC[48]
BPL[23]	BHandH[49]		tHCTH[50]
G96LYP[31,41,42]	BHandLYP[49]		
HCTH[51–53]	HSE06		
HFB[23]	M06[54]		
LC-wPBE[55–57]	M11[58]		
PBELYP[36,37,41,42]	O3LYP[34,35]		
PBEPW91[36,37,59–61]	HSE03[62]		
SLYP[25–27]	PBE0[63,64]		
SPBE[25–27]	SOGGA11[65]		
TPSSLYP1W[41,42,45]	X3LYP[41,42,66]		
mPWPBE[36,37,67]	mPW1PBE[67]		
	mPW3PBE[67]		

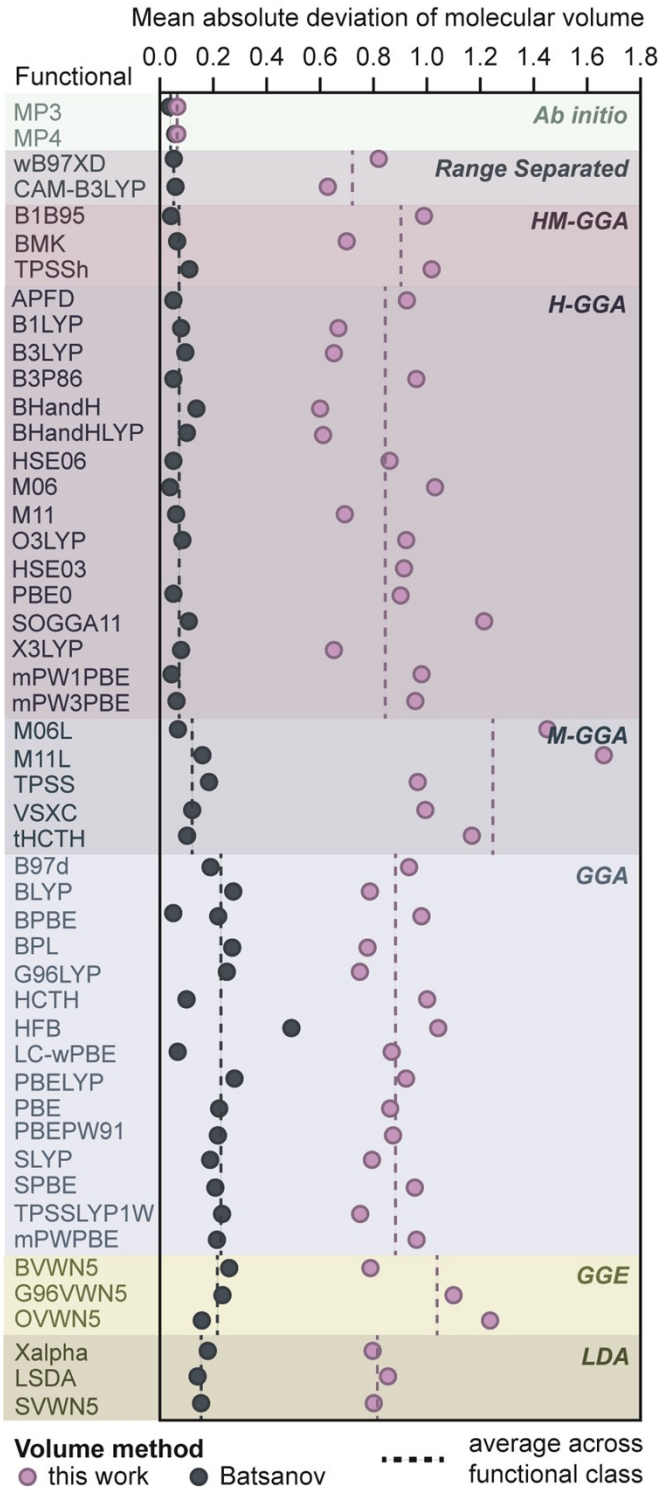

Figure S7. Mean absolute deviation of molecular volumes of the 15 test molecules, at their corresponding functional geometries. The vdW volumes are computed using the conventional rigid sphere approach, whereas the purple points are the average volume deviations of all the molecules. The dotted lines represent the average volume deviation across a functional class.

Table S4. Molecular volumes for the relevant small molecules examined in this study calculated using the van der Waals (vdW) and the STREUSEL volume calculation methods.

Molecule	vdW volume ($Å^3$)	STREUSEL volume ($Å^3$)	Difference (%)
Ne	11.25	8.260	26.58
F_2	22.03	17.25	21.70
O_2	22.97	18.77	18.28
H_2O	19.28	23.43	-21.52
N_2	23.49	19.69	16.18
CO	26.68	22.81	14.51
NH_3	22.68	26.16	-15.34
CH_4	28.15	25.08	10.91
Kr	26.52	24.26	8.522
H_2	10.49	9.690	7.626
C_2H_2	34.56	32.30	6.539
CO_2	33.21	31.49	5.179
Cl_2	39.54	37.50	5.159
SO_2	39.02	39.94	-2.358
Br_2	47.87	46.99	1.838
H_2S	29.43	29.49	-0.2039

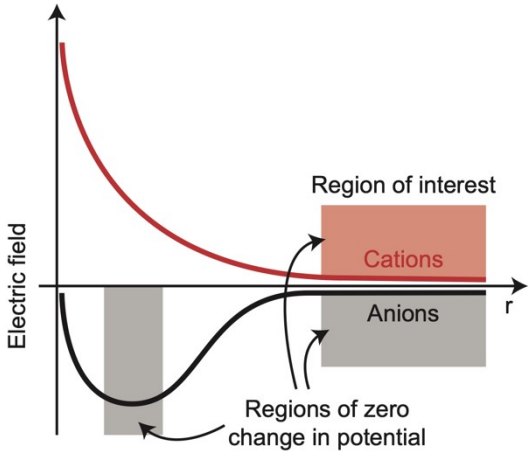

Figure S8. A schematic of the potential regions sampled by STREUSEL. Cations monotonically decrease in field as radius increases, whereas anions feature a minimum field that climbs back to 0 at large r.

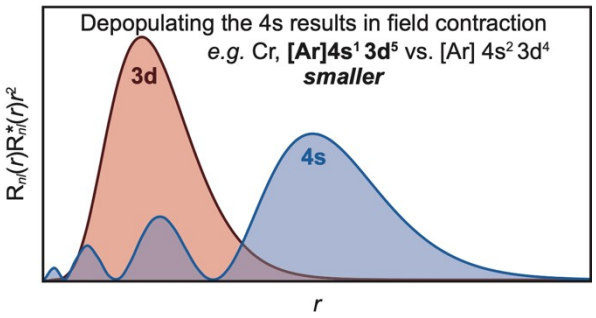

Figure S9. A schematic of the probability functions for the 3d and 4s Hydrogenic orbitals. Depopulating the higher quantum number s-orbitals generally leads to a contraction in electric field. An example is given, and a comparison of numerical radii are presented in Table S4.

Table S5. A comparison of predicted radii for the first-row transition metals with the ground state electronic structure (in bold) and an alternate non-ground state electronic structure. Depopulated s-orbitals result in contraction in radius. For Mn and above, only one spin configuration is enforceable.

Atom	Electronic configuration	Radius (Å)
Sc	**[Ar] $4s^2$ $3d^1$**	**2.40**
	[Ar] $4s^1$ $3d^2$	2.28
Ti	**[Ar] $4s^2$ $3d^2$**	**2.31**
	[Ar] $4s^1$ $3d^3$	2.20
V	**[Ar] $4s^2$ $3d^3$**	**2.27**
	[Ar] $4s^1$ $3d^4$	2.10
Cr	[Ar] $4s^2$ $3d^4$	2.21
	[Ar] $4s^1$ $3d^5$	**2.03**
Mn	**[Ar] $4s^2$ $3d^5$**	**2.01**
Fe	**[Ar] $4s^2$ $3d^6$**	**1.99**
Co	**[Ar] $4s^2$ $3d^7$**	**1.97**
Ni	**[Ar] $4s^2$ $3d^8$**	**1.93**
Cu	**[Ar] $4s^1$ $3d^{10}$**	**2.01**
Zn	**[Ar] $4s^2$ $3d^{10}$**	**1.99**

References

(1) Pyykko, P. Additive Covalent Radii for Single-, Double-, and Triple-Bonded Moleculars and Tetrahedrally Bonded Crystals: A Summary. *J. Phys. Chem. A* **2015**, *119*, 2326–2337.
(2) Pyykko, P.; Atsumi, M. Molecular Single-Bond Covalent Radii for Elements 1-118. *Chem. Eur. J.* **2009**, *15*, 186–197.
(3) Alvarez, S. A Cartography of the van Der Waals Territories. *Dalton Trans.* **2013**, *42*, 8627–8636.
(4) Cordero, B.; Gomez, V.; Platero-Prats, A. E.; Reves, M.; Echeverria, J.; Cremades, E.; Barragan, F.; Alvarez, S. Covalent Radii Revisited. *Dalton Trans.* **2008**, 2832–2838.
(5) Bragg, W. L. The Arrangement of Atoms in Crystals. *Philos. Mag.* **1920**, *40*, 169–189.
(6) Slater, J. C. Atomic Radii in Crystals. *J. Chem. Phys.* **1964**, *41*, 3199–3204.
(7) Bondi, A. Van Der Waals Volumes and Radii of Metals in Covalent Compounds. *J. Phys. Chem.* **1966**, *70*, 3006–2007.
(8) Bondi, A. Van Der Waals Volumes and Radii. *J. Phys. Chem.* **1964**, *68*, 441–451.
(9) Rahm, M.; Hoffmann, R.; Ashcroft, N. W. Atomic and Ionic Radii of Elements 1 **-96**. *Chem. Eur. J.* **2016**, *22*, 14625–14632.
(10) Batsanov, S. S. Determination of Ionic Radii from Metal Compressibilities. *J. Struct. Chem.* **2004**, *45*, 896–899.
(11) Shannon, R. D. Revised Effective Ionic Radii and Systematic Studies of Interatomic Distances in Halides and Chalcogenides. *Acta Cryst. A* **1976**, *32*, 751–767.
(12) Shannon, R. D.; Prewitt, C. T. Effective Ionic Radii in Oxides and Fluorides. *Acta. Cryst. B* **1969**, *25*, 925–946.
(13) Ouyang, R. Exploiting Ionic Radii for Rational Design of Halide Perovskites. *Chem Mater.* **2020**, *32*, 595–604.
(14) Agmon, N. Isoelectronic Theory for Cationic Radii. *J. Am. Chem. Soc.* **2017**, *139*, 15068–15073.
(15) Pauling, L. C. The Nature of the Chemical Bond and the Structure of Moleculesa Nd Crystals. In *An Introduction to Modern Structural Chemistry*; Cornell University Press: Ithaca, NY, 1960; p 644.
(16) Rahm, M.; Zeng, T.; Hoffmann, R. Electronegativity Seen as the Ground-State Average Valence Electron Binding Energy. *J. Am. Chem. Soc.* **2019**, *141*, 342–351.
(17) Frisch, M.; Schlegel, H.; Scuseria, G.; Robb, M.; Cheeseman, J.; Scalmani, G.; Barone, V.; Petersson, G.; Nakatsuji, H.; Li, X. *et al*. *Gaussian09*; Gaussian Inc. Wallingford CT, 2009.
(18) Yanai, T.; Tew, D. P.; Handy, N. C. A New Hybrid Exchange-Correlation Functional Using the Coulomb-Attenuating Method (CAM-B3LYP). *Chem. Phys. Lett.* **2004**, *393*, 51–57.
(19) Purvis, G. D.; Bartlett, R. J. A Full Coupled-cluster Singles and Doubles Model: The Inclusion of Disconnected Triples. *J. Chem. Phys.* **1982**, *76*, 1910–1918.
(20) *Advances in Chemical Physics: LeFebvre/Advances*; LeFebvre, R., Moser, C., Eds.; Advances in Chemical Physics; John Wiley & Sons, Inc.: Hoboken, NJ, USA, 1969.
(21) Scuseria, G. E.; Janssen, C. L.; Schaefer, H. F. An Efficient Reformulation of the Closed-shell Coupled Cluster Single and Double Excitation (CCSD) Equations. *J. Chem. Phys.* **1988**, *89*, 7382–7387.

(22) Scuseria, G. E.; Schaefer, H. F. Is Coupled Cluster Singles and Doubles (CCSD) More Computationally Intensive than Quadratic Configuration Interaction (QCISD)? *J. Chem. Phys.* **1989**, *90*, 3700–3703.
(23) Becke, A. D. Density-functional Thermochemistry. IV. A New Dynamical Correlation Functional and Implications for Exact-exchange Mixing. *J. Chem. Phys.* **1996**, *104*, 1040–1046.
(24) Vosko, S. H.; Wilk, L.; Nusair, M. Accurate Spin-Dependent Electron Liquid Correlation Energies for Local Spin Density Calculations: A Critical Analysis. *Can. J. Phys.* **1980**, *58*, 1200–1211.
(25) Slater, J. C. *Quantum Theory of Molecules and Solids*; International series in pure and applied physics; McGraw-Hill: New York, 1963.
(26) Hohenberg, P.; Kohn, W. Inhomogeneous Electron Gas. *Phys. Rev.* **1964**, *136*, B864–B871.
(27) Kohn, W.; Sham, L. J. Self-Consistent Equations Including Exchange and Correlation Effects. *Phys. Rev.* **1965**, *140*, A1133–A1138.
(28) Chai, J.-D.; Head-Gordon, M. Long-Range Corrected Hybrid Density Functionals with Damped Atom–Atom Dispersion Corrections. *Phys. Chem. Chem. Phys.* **2008**, *10*, 6615.
(29) Pople, J. A.; Binkley, J. S.; Seeger, R. Theoretical Models Incorporating Electron Correlation. *Int. J. Quant. Chem.* **2009**, *10*, 1–19.
(30) Pople, J. A.; Seeger, R.; Krishnan, R. Variational Configuration Interaction Methods and Comparison with Perturbation Theory. *Int. J. Quant. Chem.* **2009**, *12*, 149–163.
(31) Gill, P. M. W. A New Gradient-Corrected Exchange Functional. *Mol. Phys.* **1996**, *89*, 433–445.
(32) Krishnan, R.; Pople, J. A. Approximate Fourth-Order Perturbation Theory of the Electron Correlation Energy. *Int. J. Quant. Chem.* **1978**, *14*, 91–100.
(33) Krishnan, R.; Frisch, M. J.; Pople, J. A. Contribution of Triple Substitutions to the Electron Correlation Energy in Fourth Order Perturbation Theory. *J. Chem. Phys.* **1980**, *72*, 4244–4245.
(34) Handy, N. C.; Cohen, A. J. Left-Right Correlation Energy. *Mol. Phys.* **2001**, *99*, 403–412.
(35) Hoe, W.-M.; Cohen, A. J.; Handy, N. C. Assessment of a New Local Exchange Functional OPTX. *Chem. Phys. Lett.* **2001**, *341*, 319–328.
(36) Perdew, J. P.; Burke, K.; Ernzerhof, M. Generalized Gradient Approximation Made Simple. *Phys. Rev. Lett.* **1996**, *77*, 3865–3868.
(37) Perdew, J. P.; Burke, K.; Ernzerhof, M. Generalized Gradient Approximation Made Simple [Phys. Rev. Lett. 77, 3865 (1996)]. *Phys. Rev. Lett.* **1997**, *78*, 1396–1396.
(38) Austin, A.; Petersson, G. A.; Frisch, M. J.; Dobek, F. J.; Scalmani, G.; Throssell, K. A Density Functional with Spherical Atom Dispersion Terms. *J. Chem. Theory Comput.* **2012**, *8*, 4989–5007.
(39) Zhao, Y.; Truhlar, D. G. A New Local Density Functional for Main-Group Thermochemistry, Transition Metal Bonding, Thermochemical Kinetics, and Noncovalent Interactions. *J. Chem. Phys.* **2006**, *125*, 194101.
(40) Grimme, S. Semiempirical GGA-Type Density Functional Constructed with a Long-Range Dispersion Correction. *J. Comput. Chem.* **2006**, *27*, 1787–1799.
(41) Lee, C.; Yang, W.; Parr, R. G. Development of the Colle-Salvetti Correlation-Energy Formula into a Functional of the Electron Density. *Phys. Rev. B* **1988**, *37*, 785–789.

(42) Miehlich, B.; Savin, A.; Stoll, H.; Preuss, H. Results Obtained with the Correlation Energy Density Functionals of Becke and Lee, Yang and Parr. *Chem. Phys. Lett.* **1989**, *157*, 200–206.
(43) Boese, A. D.; Martin, J. M. L. Development of Density Functionals for Thermochemical Kinetics. *J. Chem. Phys.* **2004**, *121*, 3405–3416.
(44) Peverati, R.; Truhlar, D. G. M11-L: A Local Density Functional That Provides Improved Accuracy for Electronic Structure Calculations in Chemistry and Physics. *J. Phys. Chem. Lett.* **2012**, *3*, 117–124.
(45) Tao, J.; Perdew, J. P.; Staroverov, V. N.; Scuseria, G. E. Climbing the Density Functional Ladder: Nonempirical Meta–Generalized Gradient Approximation Designed for Molecules and Solids. *Phys. Rev. Lett.* **2003**, *91,* 146401.
(46) Staroverov, V. N.; Scuseria, G. E.; Tao, J.; Perdew, J. P. Comparative Assessment of a New Nonempirical Density Functional: Molecules and Hydrogen-Bonded Complexes. *J. Chem. Phys.* **2003**, *119*, 12129–12137.
(47) Staroverov, V. N.; Scuseria, G. E.; Tao, J.; Perdew, J. P. Erratum: "Comparative Assessment of a New Nonempirical Density Functional: Molecules and Hydrogen-Bonded Complexes" [J. Chem. Phys. 119, 12129 (2003)]. *J. Chem. Phys.* **2004**, *121*, 11507.
(48) Van Voorhis, T.; Scuseria, G. E. A Novel Form for the Exchange-Correlation Energy Functional. *J. Chem. Phys.* **1998**, *109*, 400–410.
(49) Becke, A. D. A New Mixing of Hartree–Fock and Local Density-functional Theories. *J. Chem. Phys.* **1993**, *98*, 1372–1377.
(50) Boese, A. D.; Handy, N. C. New Exchange-Correlation Density Functionals: The Role of the Kinetic-Energy Density. *J. Chem. Phys.* **2002**, *116*, 9559–9569.
(51) Boese, A. D.; Handy, N. C. A New Parametrization of Exchange–Correlation Generalized Gradient Approximation Functionals. *J. Chem. Phys.* **2001**, *114*, 5497–5503.
(52) Boese, A. D.; Doltsinis, N. L.; Handy, N. C.; Sprik, M. New Generalized Gradient Approximation Functionals. *J. Chem. Phys.* **2000**, *112*, 1670–1678.
(53) Hamprecht, F. A.; Cohen, A. J.; Tozer, D. J.; Handy, N. C. Development and Assessment of New Exchange-Correlation Functionals. *J. Chem. Phys.* **1998**, *109*, 6264–6271.
(54) Zhao, Y.; Truhlar, D. G. The M06 Suite of Density Functionals for Main Group Thermochemistry, Thermochemical Kinetics, Noncovalent Interactions, Excited States, and Transition Elements: Two New Functionals and Systematic Testing of Four M06-Class Functionals and 12 Other Functionals. *Theor. Chem. Acc.* **2008**, *120*, 215–241.
(55) Vydrov, O. A.; Scuseria, G. E. Assessment of a Long-Range Corrected Hybrid Functional. *J. Chem. Phys.* **2006**, *125*, 234109.
(56) Vydrov, O. A.; Scuseria, G. E.; Perdew, J. P. Tests of Functionals for Systems with Fractional Electron Number. *J. Chem. Phys.* **2007**, *126*, 154109.
(57) Vreven, T.; Frisch, M. J.; Kudin, K. N.; Schlegel, H. B.; Morokuma, K. Geometry Optimization with QM/MM Methods II: Explicit Quadratic Coupling. *Mol. Phys.* **2006**, *104*, 701–714.
(58) Peverati, R.; Truhlar, D. G. Improving the Accuracy of Hybrid Meta-GGA Density Functionals by Range Separation. *J. Phys. Chem. Lett.* **2011**, *2*, 2810–2817.
(59) Perdew, J. P.; Chevary, J. A.; Vosko, S. H.; Jackson, K. A.; Pederson, M. R.; Singh, D. J.; Fiolhais, C. Atoms, Molecules, Solids, and Surfaces: Applications of the Generalized Gradient Approximation for Exchange and Correlation. *Phys. Rev. B* **1992**, *46*, 6671–6687.

(60) Perdew, J. P.; Chevary, J. A.; Vosko, S. H.; Jackson, K. A.; Pederson, M. R.; Singh, D. J.; Fiolhais, C. Erratum: Atoms, Molecules, Solids, and Surfaces: Applications of the Generalized Gradient Approximation for Exchange and Correlation. *Phys. Rev. B* **1993**, *48*, 4978–4978.
(61) *Electronic Density Functional Theory: Recent Progress and New Directions*; Dobson, J. F., Vignale, G., Das, M. P., Eds.; Plenum Press: New York, 1998.
(62) Heyd, J.; Scuseria, G. E.; Ernzerhof, M. Hybrid Functionals Based on a Screened Coulomb Potential. *J. Chem. Phys.* **2003**, *118*, 8207–8215.
(63) Adamo, C.; Barone, V. Toward Reliable Density Functional Methods without Adjustable Parameters: The PBE0 Model. *J. Chem. Phys.* **1999**, *110*, 6158–6170.
(64) Ernzerhof, M.; Scuseria, G. E. Assessment of the Perdew–Burke–Ernzerhof Exchange-Correlation Functional. *J. Chem. Phys.* **1999**, *110*, 5029–5036.
(65) Peverati, R.; Zhao, Y.; Truhlar, D. G. Generalized Gradient Approximation That Recovers the Second-Order Density-Gradient Expansion with Optimized Across-the-Board Performance. *J. Phys. Chem. Lett.* **2011**, *2*, 1991–1997.
(66) Xu, X.; Goddard, W. A. From The Cover: The X3LYP Extended Density Functional for Accurate Descriptions of Nonbond Interactions, Spin States, and Thermochemical Properties. *Proc. Nat. Acad. Sci. USA* **2004**, *101*, 2673–2677.
(67) Adamo, C.; Barone, V. Exchange Functionals with Improved Long-Range Behavior and Adiabatic Connection Methods without Adjustable Parameters: The MPW and MPW1PW Models. *J. Chem. Phys.* **1998**, *108*, 664–675.